

Mechanical Response of Semi-Brittle Ceramics Subjected to Tension-Compression State. Part I: Theoretical Modeling

TOMASZ SADOWSKI*
Technische Universität München
Lehrstuhl A für Mechanik
80333 München
Arcisstrasse 21, Germany

ABSTRACT: This article discusses the construction of constitutive equations for the quasi-static deformation process of semi-brittle materials from the onset to the state preceding final failure. The simple connection between mesomechanical and phenomenological modelling of damage is possible. The generalization of the damage measurement idea by unloading modulus [31] allows one to follow the whole non-linear unloading process in the multi-axial state of stress, specifying all mechanisms contained in it.

1. INTRODUCTION

THE EXISTENCE OF cracks, pores and other defects within solids diametrically changes the material response to applied load. Many effective continuum models have been proposed to estimate mechanical properties of materials (for example, References [1–9]). In the case of semi-brittle ceramics, a small amount of plasticity also influences the total material response [10–12].

The aim of this paper is to follow the two-dimensional, quasi-static deformation process (tension-compression) of semi-brittle ceramics. The mechanical response of polycrystalline continua, weakened by a set of slits, is modelled by application mean field theories [13–15]. According to the experimental results (MgO) [16–18], limited plastic flow is created by dislocation motion within the range of grains of the representative volume element. Microcracks are initiated by Zener-Stroh's mechanism and propagate mainly intergranularly, along grain boundaries (zig-zag cracks), leading to final failure of the material.

*On leave from Technical University of Lublin, Faculty of Civil and Sanitary Engineering, ul. Nadbystrzycka 40, 20-618 Lublin, Poland.

This study focuses mainly on the description of gradual material degradation including micromechanically based estimation of current elastic properties. The degradation process is related not only to numbers of defects, like in many models, but is also strongly dependent on the real crack shapes and their distribution within the unit cell. Smooth transition from uniaxial tension to uniaxial compression by the two dimensional states is analysed with specification of particular modes of crack shapes and their distribution within the unit cell, up to the state preceding final failure.

2. MEAN FIELD MODEL

To describe material behaviour, it is necessary to consider the problem in two scales (see, for example, References [1-3,7,10-15]). In macroscale, the material behaves as a continuum and we denote the states of stress and strain by $\underline{\sigma}$ and $\underline{\epsilon}$, respectively. In mesoscale, the solid is inhomogeneous and anisotropic. In this case, local values of the stress and strain ($\underline{\sigma}', \underline{\epsilon}'$) describe different defects existent in grains or at the grain boundaries. Connection of these two scales is possible by an averaging procedure over the unit cell.

$$\underline{\sigma} = \frac{1}{A} \int_A \underline{\sigma}' dA, \quad \underline{\epsilon} = \frac{1}{A} \int_A \underline{\epsilon}' dA \quad (1)$$

where A is the area of the unit cell. In general, the strain components of polycrystalline materials can be decomposed into the elastic part, $\underline{\epsilon}^e$, and parts associated with defect (dislocation bands, cracks, voids or inclusions, etc.) creation $\underline{\epsilon}^d(i)$:

$$\underline{\epsilon} = (1 - f)\underline{\epsilon}^e + \sum_{N_i} f_d^{(i)} \underline{\epsilon}^d(i) \quad (2)$$

where f and $f_d^{(i)}$ are the surface area density of all defects (A_d), and i th defects ($A_d^{(i)}$), respectively. N_i denotes the number of defects within the unit cell. The superposition in Equation (2) is possible with the application of the Taylor model.

In the most general case, the continuous damage process is defined by constitutive relations expressed as a tensor function of two variables: the stress tensor $\underline{\sigma}$ and damage tensor $\underline{\omega}$ (see, for example, Reference [19]), i.e.

$$\underline{\epsilon} = \underline{\epsilon}(\underline{\sigma}, \underline{\omega}) \quad (3)$$

where $\underline{\epsilon}$ is the strain tensor; $\underline{\omega}$ has been assumed to be the only internal parameter. When the deformation process is under consideration, an evolution equation

should be postulated for the damage parameter $\underline{\omega}$

$$\dot{\underline{\omega}} = \dot{\underline{\omega}}(\underline{\sigma}, \underline{\omega}) \quad (4)$$

($\dot{}$) means the change of damage in time.

In the case of a quasi-static increase of the external load of a material, it would seem reasonable to postulate a steady change of damage with time, i.e.

$$\dot{\underline{\omega}} = \text{const.} \quad (5)$$

Solving Equation (4) with this assumption, a direct relation between the tensors of damage and stress can be obtained, namely

$$\underline{\omega} = \underline{\omega}(\underline{\sigma}) \quad (6)$$

Thus, the specified set of Equations (3)–(6) creates a dual description for damaging materials in relation to Reference [9].

A detailed discussion of constitutive equations and damage criteria, as well as failure, is presented in Reference [20]. Here, we limit our consideration to the analysis of the overall (macro) compliance tensor $\underline{\underline{S}}$, built up on the basis of quasi-static changes within the unit cell, reflecting degradation of the internal structure of the polycrystalline material. According to Equations (2) and (3), we have

$$\underline{\underline{\epsilon}} = \underline{\underline{S}}(\underline{\sigma}, \underline{\omega}) : \underline{\sigma} \quad (7)$$

and (e.g., References [3] and [21])

$$\underline{\underline{S}}(\underline{\sigma}, \underline{\omega}) = \underline{\underline{S}}^0 + \underline{\underline{S}}^*(\underline{\sigma}, \underline{\omega}) \quad (8)$$

where $\underline{\underline{S}}^0$ is the compliance of the virgin material and $\underline{\underline{S}}^*$ is the compliance attributable to the propagation of all microdefects N_i .

3. MODELLING OF SEMI-BRITTLE CERAMICS UNDER LOADING PROCESS

The quasi-static deformation process of MgO polycrystalline ceramic was theoretically investigated for a uniaxial state of tension [10,11] and compression [12]. The present paper proposes a unified description of the material behaviour for a two-dimensional state of stress (Figure 1) obeying the above two limiting cases.

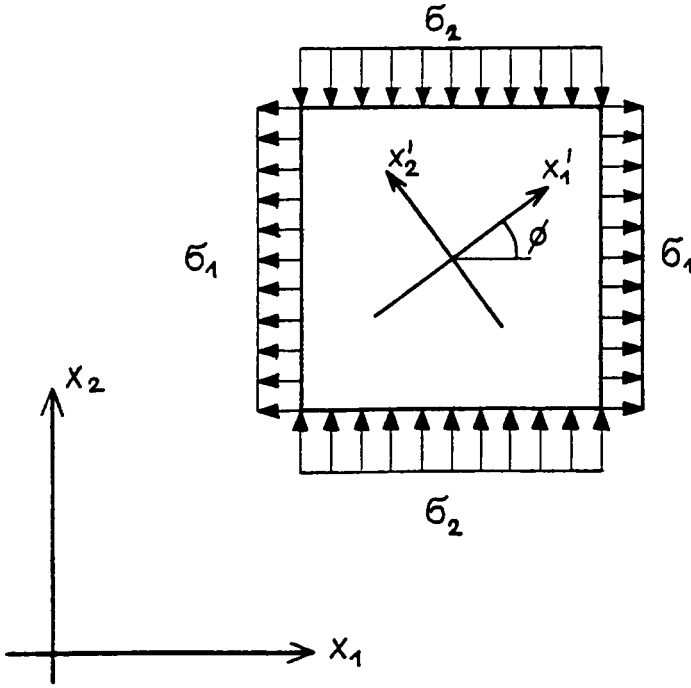


Figure 1. Schematic diagram of the considered problem.

In the matrix notation, the constitutive relations (7) simplify to:

$$\begin{pmatrix} \epsilon_1 \\ \epsilon_2 \\ \epsilon_6 \end{pmatrix} = \begin{pmatrix} S_{11} & S_{12} & S_{16} \\ S_{21} & S_{22} & S_{26} \\ S_{61} & S_{62} & S_{66} \end{pmatrix} \begin{pmatrix} \sigma_1 \\ \sigma_2 \\ \sigma_6 \end{pmatrix} \tag{9}$$

when the Voigt's description was applied. Further [22], the deformation process will be limited to so-called proportional loading defined by

$$\sigma_2 = q, \quad \sigma_1 = kq \quad \text{and} \quad \sigma_{12} = 0 \tag{10}$$

where k is a constant. Under these assumptions, the influence of the q increase on the particular form of the compliance tensor S^* will be investigated.

3.1 Slip Phase

Experimental evidence [16,17] shows that after the purely elastic phase, dislocation sources activate within grains, creating conjugate slip systems (100)

$\langle 110 \rangle$; they pile up to grain boundaries, but cannot cross them, in general, because of the strong energetic barrier to easy glide. In this way, surrounding grains resist free deformation of crystals with activated slip systems. According to Reference [12], the following components of S are different from zero.

$$S_{11}^{*(s)} = \frac{N_s}{\pi G_0(1 - b_1)} \int_{D_m}^{D_M} \int_{\beta_1}^{\beta_2} \left[-\sin(\beta) \cos(\beta) - \frac{\tau_{so}}{\sigma_1 + \sigma_2} \right] \alpha_{ij}(\beta) p_2(D) d\beta dD \tag{11}$$

$$S_{22}^{*(s)} = \frac{N_s}{\pi G_0(1 - b_1)} \int_{D_m}^{D_M} \int_{\beta_1}^{\beta_2} \left[\sin(\beta) \cos(\beta) - \frac{\tau_{so}}{\sigma_1 + \sigma_2} \right] \alpha_{ij}(\beta) p_2(D) d\beta dD \tag{12}$$

$$S_{11}^{*(s)} = -S_{22}^{*(s)}, \quad S_{12}^{*(s)} = -S_{21}^{*(s)} \tag{13}$$

where N_s is the number of grains with conjugate slip systems inside the unit cell, τ_{so} is the lattice resistance to dislocation glide, $p_2(D)$ is the grain size distribution function, D_m and D_M are the smallest and largest grains sizes, respectively, G_0 is the Kirchhoff modulus of the virgin material, and b_1 is the coefficient connected with the shape of the grains. β is the angle of the slip band inclination to the axis x_1 , whereas $\beta_1 < \beta < \beta_2$ denotes the fan of N_s grains.

3.2 Mesocrack Creation and Development

The mechanism of crack initiation is strictly connected to the grain boundary properties of the material. Namely, the surface energy γ_{gb} along the grain boundaries, considerably lower in comparison to pure crystals γ_g [16,17,23], creates profitable conditions to the Zener-Stroh crack initiation. A minimal value of the shear resolved stress τ_{ec} potent enough to produce microcracks can be estimated [10–12]:

$$\tau_{ec}^{min} = \left\{ \frac{3\pi\gamma_{gb}G_0}{8(1 - \nu_0)d} \right\}^{1/2} \tag{14}$$

where G_0 is the shear modulus of the virgin material, and d is the pile up length.

In order to describe the microcrack development phase, let us consider a single straight slit in the local coordinate system $x'_1x'_2$ inclined to the global one under angle ϕ . Depending on the state of stress and ϕ , the crack can be opened or closed. In the first case, it propagates under mixed mode

$$\frac{1 - \nu_0}{E} (K_I^2 + K_{II}^2) = \gamma_{gb} \tag{15}$$

where ν_0 is the Poisson coefficient of the virgin material. The closed slit is subjected to action of the shear stress τ_s , creating displacement discontinuity

$$\tau_s = \frac{1}{2}(\sigma_2 - \sigma_1) \sin(2\phi) - \mu[\sigma_1 \sin^2(\phi) + \sigma_2 \cos^2(\phi)] \tag{16}$$

and growth under mode II. Thus, in the unit cell we have closed microcracks, open and sliding slits and mesocracks occupying straight segments of grain boundaries [see Figure 2, valid for Equation (10)].

The mesocracks are opened when the local value of the stress component, normal to the crack face, is positive. Then the total influence of the $N_m^{(o)}$ opened slits on the overall material response is equal (see Appendix A):

$$S_{ij}^{*(o)} = \frac{2\pi}{AE_0} N_m^{(o)} \int_{\phi_1^{(o)}}^{\phi_2^{(o)}} \int_{D_m} M_{ij}^{(o)} \left(\frac{D}{4}\right)^2 p_1(\phi) p_2(D) dD d\phi \tag{17}$$

where $p_1(\phi)$ and $p_2(D)$ are the inclination of mesocrack and grain distribution

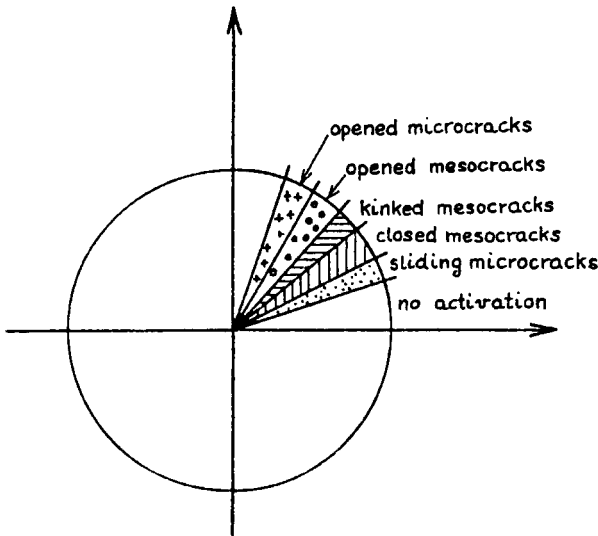


Figure 2. Domains of the crack response within the unit cell for the state preceding final failure.

functions, respectively, and $M_{ij}^{(o)}$ is the two-dimensional matrix (Appendix A):

$$\{M_{ij}^{(o)}\} = \begin{Bmatrix} M_{11}^{(o)} & M_{12}^{(o)} & M_{16}^{(o)} \\ M_{21}^{(o)} & M_{22}^{(o)} & M_{26}^{(o)} \\ M_{61}^{(o)} & M_{62}^{(o)} & M_{66}^{(o)} \end{Bmatrix} = \begin{Bmatrix} \sin^2 \phi(2 - 3 \cos^2 \phi) & 3 \sin^2 \phi \cos^2 \phi & 0 \\ \cos^2 \phi(1 - \cos^2 \phi) & \cos^2 \phi(1 + \cos^2 \phi) & 0 \\ -\frac{1}{2} \sin 2\phi(1 + 2 \sin^2 \phi) & -\frac{1}{2} \sin 2\phi(1 + 2 \cos^2 \phi) & 0 \end{Bmatrix} \quad (18)$$

whereas $\phi_{\varepsilon_1}^{(o)} < \phi^{(o)} < \phi_{\varepsilon_2}^{(o)}$ denotes the fan of $N_m^{(o)}$ cracks.

Similarly, generalizing Reference [12], the closed slits $N_m^{(c)}$ change the material response according to (see Appendix B):

$$S_{ij}^{*(c)} = \frac{2\pi}{AE_0} N_m^{(c)} \int_{\phi_{\varepsilon_1}^{(c)}}^{\phi_{\varepsilon_2}^{(c)}} \int_{D_m} M_{ij}^{(c)} \left(\frac{D}{4}\right)^2 p_1(\phi)p_2(D) dDd\phi \quad (19)$$

where $M_{ij}^{(c)}$ is the following matrix

$$\{M_{ij}^{(c)}\} = \begin{Bmatrix} M_{11}^{(c)} & M_{12}^{(c)} & M_{16}^{(c)} \\ M_{21}^{(c)} & M_{22}^{(c)} & M_{26}^{(c)} \\ M_{61}^{(c)} & M_{62}^{(c)} & M_{66}^{(c)} \end{Bmatrix} = \begin{Bmatrix} -\frac{1}{4} \sin^2 2\phi + \mu \sin^3 \phi \cos \phi & \frac{1}{4} \sin^2 2\phi - \mu \sin \phi \cos^3 \phi & 0 \\ \frac{1}{4} \sin^2 2\phi + \mu \sin^3 \phi \cos \phi & -\frac{1}{4} \sin^2 2\phi + \mu \sin \phi \cos^3 \phi & 0 \\ \frac{1}{4} \sin 4\phi + \mu \sin^2 \phi \cos 2\phi & -\frac{1}{4} \sin 4\phi + \mu \cos^2 \phi \cos 2\phi & 0 \end{Bmatrix} \quad (20)$$

3.3 Mesocrack Deflection (Kinking)

The mesocracks, which occupy the straight segment of the grain boundary, can deflect, changing the direction of their propagation (toughening mechanism). We consider the intergranular mode of slit propagation (see experimental results [16,18,23]) since the surface energy of the grain boundaries γ_{gb} is substantially less [23] in comparison to the surface energy of pure crystals γ_c .

According to References [7], [12] and [24], in the case of simple compression, a kinking crack is described by the introduction of thin straight mesocracks endowed with frictional resistance which nucleate tension cracks at their tips [Figure 3(a)]. For the two-dimensional case, where opened mesocracks also exist within the unit cell, one can simply generalize this model. Namely, a zig-zag crack can be approximated by an equivalent crack of length $2l$, subjected to a pair of concentrated forces F and F^* created by sliding and opening effects of the mesocrack [Figure 3(b)]. Their values are equal:

$$F = \begin{cases} \frac{D}{2}\tau_s & \text{for closed mesocracks} \\ \frac{D}{2}\sigma'_6 & \text{for opened mesocracks} \end{cases} \quad (21)$$

$$F^* = \begin{cases} 0 & \text{for closed mesocracks} \\ \frac{D}{2}\sigma'_2 & \text{for opened mesocracks} \end{cases} \quad (22)$$

Here, σ'_2 and σ'_6 denote local values of the state of stress. The forces F and F^* influence the stress intensity factors at the tips Q and Q' as follows:

$$k_I = -\frac{D}{2} \left\{ \begin{array}{l} \tau_s \sin(\theta) \\ \tau_s \sin(\theta) + \tau'_2 \cos(\theta) \end{array} \right\} \left| [\pi(l + l^*)]^{1/2} \right. \\ \left. - (\pi l)^{1/2} \frac{1}{2} [\sigma_2 + \sigma_1 + (\sigma_1 - \sigma_2) \cos 2(\theta + \phi)] \right\} \quad (23)$$

$$k_{II} = \frac{D}{2} \left\{ \begin{array}{l} \tau_s \cos(\theta) \\ \tau_s \cos(\theta) + \tau'_2 \sin(\theta) \end{array} \right\} \left| [\pi(l + l^*)]^{1/2} \right. \\ \left. - (\pi l)^{1/2} \frac{1}{2} [(\sigma_1 - \sigma_2) \sin 2(\theta + \phi)] \right\} \quad (24)$$

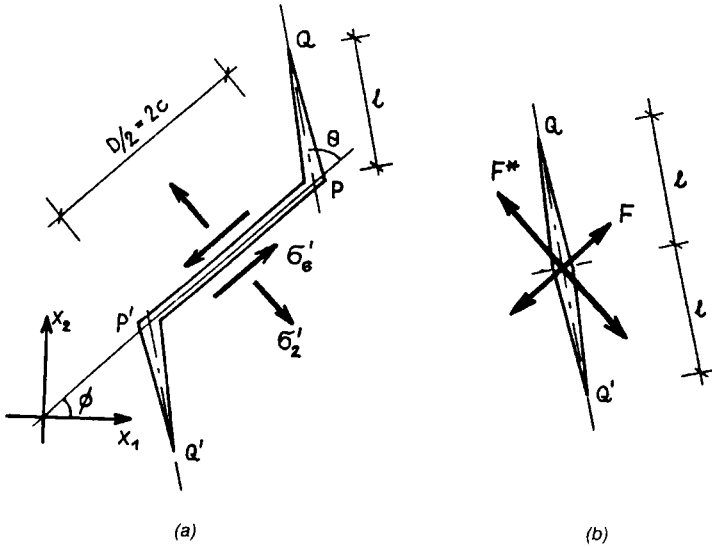


Figure 3. (a) Straight mesocrack PP' with tension cracks PQ and P'Q' and (b) equivalent crack.

The upper expressions in the braces are related to closed mesocracks, whereas the lower expressions are related to opened ones. The second parts of Equations (23) and (24) present an influence of external load; $l + l^*$ is the equivalent kink length [24].

Under the above assumptions, the overall material response can be described for opened mesocracks, $\hat{N}_m^{(o)}$, potent enough for kink creation:

$$\hat{S}_{ij}^{*(o)} = \frac{\pi}{E_0} \hat{N}_m^{(o)} \int_{l_{k_1}^{(o)}}^{l_{k_2}^{(o)}} p_{k_1}(\bar{l}) \int_{\theta_{k_1}^{(o)} + \phi_{k_1}^{(o)}}^{\theta_{k_2}^{(o)} + \phi_{k_2}^{(o)}} \hat{M}_{ij}^{(o)} p_{k_2}(\theta + \phi) \bar{l} d\bar{l} d(\theta + \phi) \quad (25)$$

where matrix $\hat{M}_{ij}^{(o)}$ is equal (see Appendix C):

$$\begin{aligned} \{\hat{M}_{ij}^{(o)}\} &= \begin{Bmatrix} \hat{M}_{11}^{(o)} & \hat{M}_{12}^{(o)} & \hat{M}_{16}^{(o)} \\ \hat{M}_{21}^{(o)} & \hat{M}_{22}^{(o)} & \hat{M}_{26}^{(o)} \\ \hat{M}_{61}^{(o)} & \hat{M}_{62}^{(o)} & \hat{M}_{66}^{(o)} \end{Bmatrix} \\ &= \begin{Bmatrix} \sin \phi \cos (2\theta) \sin (\theta + \phi) & \cos \phi \sin (2\theta) \sin (\theta + \phi) & 0 \\ -\sin \phi \sin (2\theta) \cos (\theta + \phi) & \cos \phi \cos (2\theta) \cos (\theta + \phi) & 0 \\ -\sin \phi \cos (3\theta + \phi) & -\cos \phi \sin (3\theta + \phi) & 0 \end{Bmatrix} \quad (26) \end{aligned}$$

In Equation (25), p_{k_1} and p_{k_2} are the tension cracks length and the inclination angle distribution function, respectively. $\bar{l}_{k_1}^{(o)} \leq \bar{l} \leq \bar{l}_{k_2}^{(o)}$ characterize the fan of the length, whereas $\theta_{k_1}^{(o)} + \phi_{k_1}^{(o)} \leq \theta + \phi \leq \theta_{k_2}^{(o)} + \phi_{k_2}^{(o)}$ characterizes the fan of the kinked crack inclination.

For closed mesocracks $\hat{N}_m^{(c)}$ forming kinks at their ends, we have (see Reference [12] and Appendix D):

$$\hat{S}_{ij}^{*(c)} = \frac{\pi}{E_0} \hat{N}_m^{(c)} \int_{\bar{l}_{k_1}^{(c)}}^{\bar{l}_{k_2}^{(c)}} p_{k_1}(\bar{l}) \int_{\theta_{k_1}^{(c)} + \phi_{k_1}^{(c)}}^{\theta_{k_2}^{(c)} + \phi_{k_2}^{(c)}} \hat{M}_{ij}^{(c)} p_{k_2}(\theta + \phi) \bar{l} d\bar{l} d(\theta + \phi) \quad (27)$$

and

$$\{\hat{M}_{ij}^{(c)}\} = \begin{pmatrix} \hat{M}_{11}^{(c)} & \hat{M}_{12}^{(c)} & \hat{M}_{16}^{(c)} \\ \hat{M}_{21}^{(c)} & \hat{M}_{22}^{(c)} & \hat{M}_{26}^{(c)} \\ \hat{M}_{61}^{(c)} & \hat{M}_{62}^{(c)} & \hat{M}_{66}^{(c)} \end{pmatrix}$$

$$= \begin{pmatrix} \sin^2 \phi \cos \phi \sin(\theta + \phi) [\text{ctg} \phi - \mu] & \cos^3 \phi \sin(\theta + \phi) [\text{tg} \phi - \mu] & 0 \\ -\sin^3 \phi \cos(\theta + \phi) [\text{ctg} \phi - \mu] & \sin \phi \cos^2 \phi \cos(\theta + \phi) [\text{tg} \phi - \mu] & 0 \\ -\sin^2 \phi \cos(\theta + 2\phi) [\text{ctg} \phi - \mu] & \cos^2 \phi \cos(\theta + 2\phi) [\text{tg} \phi - \mu] & 0 \end{pmatrix} \quad (28)$$

$\bar{l}_{k_1}^{(c)} \leq \bar{l} \leq \bar{l}_{k_2}^{(c)}$ characterizes the fan of the length, whereas $\theta_{k_1}^{(c)} + \phi_{k_1}^{(c)} \leq \theta + \phi \leq \theta_{k_2}^{(c)} + \phi_{k_2}^{(c)}$ characterizes the fan of kinked crack inclination.

The last component of the compliance S^* is connected with the closing or opening effect of kinks under an external loading or unloading process. The amount of change can be estimated from (see Appendix E):

$$\begin{aligned} \bar{S}_{ij}^* = & \frac{\pi D^2}{16AE_0} \left[\hat{N}_m^{(o)} \int_{\bar{l}_{k_1}^{(o)}}^{\bar{l}_{k_2}^{(o)}} p_{k_1}(\bar{l}) \int_{\theta_{k_1}^{(o)} + \phi_{k_1}^{(o)}}^{\theta_{k_2}^{(o)} + \phi_{k_2}^{(o)}} \bar{M}_{ij} p_{k_2}(\theta + \phi) \bar{l}^2 d\bar{l} d(\theta + \phi) \right. \\ & \left. + \hat{N}_m^{(c)} \int_{\bar{l}_{k_1}^{(c)}}^{\bar{l}_{k_2}^{(c)}} p_{k_1}(\bar{l}) \int_{\theta_{k_1}^{(c)} + \phi_{k_1}^{(c)}}^{\theta_{k_2}^{(c)} + \phi_{k_2}^{(c)}} \bar{M}_{ij} p_{k_2}(\theta + \phi) \bar{l}^2 d\bar{l} d(\theta + \phi) \right] \quad (29) \end{aligned}$$

where \bar{M}_{ij} is the following matrix:

$$\{\bar{M}_{ij}\} = \begin{pmatrix} \bar{M}_{11} & \bar{M}_{12} & \bar{M}_{16} \\ \bar{M}_{21} & \bar{M}_{22} & \bar{M}_{26} \\ \bar{M}_{61} & \bar{M}_{62} & \bar{M}_{66} \end{pmatrix}$$

$$= \begin{pmatrix} \sin^2(\theta + \phi) & 0 & 0 \\ 0 & \cos^2(\theta + \phi) & 0 \\ -\frac{1}{2} \sin 2(\theta + \phi) & -\frac{1}{2} \sin 2(\theta + \phi) & 0 \end{pmatrix} \quad (30)$$

3.4 Total Overall Response

The total overall response, defined by Equation (8), will be calculated by the summation of all previously discussed components: Equations (11)–(13), (17), (19), (25), (27) and (29). Finally, we gain

$$S_{ij}(\underline{\sigma}) = S_{ij}^0 + S_{ij}^{*(s)} + S_{ij}^{*(o)} + S_{ij}^{*(c)} + \hat{S}_{ij}^{*(o)} + \hat{S}_{ij}^{*(c)} + \bar{S}_{ij}^* \quad (31)$$

Equation (31) shows a rather complicated structure of the compliance tensor, postulated for the Taylor model. It strongly depends on the inclination fans of existing mesocracks and the propagation mode of the secondary cracks. They are strictly connected with the actual state of stress (σ_1 , σ_2).

In the most general case, formula (31) should be extended to a description of the interaction effects between cracks [20], but these effects were observed only for two-phase ceramics like $\text{Al}_2\text{O}_3/\text{ZrO}_2$ or SiC/TiB_2 [25]. Theoretical derivations also lead to the conclusion that the toughness enhancement by shielding effect is almost exactly counterbalanced by the reduction of toughness in the isotropically microcracked material (References [26]–[28] and others).

4. MODELLING OF SEMI-BRITTLE CERAMICS UNDER UNLOADING PROCESS

Let us define the unloading process of the material in the two-dimensional stress state. We assume that this process begins when:

1. The stress components do not increase.
2. At least one of the two components σ_1 and σ_2 decrease.

A lot of material models with internal degradation (e.g., References [4] and [28]) postulate total reversibility of the strain during unloading. However, experimental observations suggest that some amount of strain remains after complete unloading; this was noted in References [8] and [29], and theoretically described for uniaxial compression of semi-brittle MgO ceramics in Reference [12]. In general, the value of “back strains” depends on the (1) roughness of the mesocrack surfaces and (2) the real crack shape (zig-zag deflection). One can simply estimate the strains for any state of the considered process using decomposition into independent components of the compliance tensor \underline{S} [Equation (31)]. Additionally, we postulate that during unloading:

1. The plastic strains do not change.
2. The mesocracks can remain closed or opened depending on the local state of stress $\underline{\sigma}'$.
3. The kinks of the mesocracks start to open, close or propagate in relation to $\underline{\sigma}'$.

Thus, the compliance tensor for unloading paths of the material response can be calculated

$$S_{ij}^u(\underline{\sigma}) = S_{ij}^o + S_{ij}^{u*(o)} + S_{ij}^{u*(c)} + \hat{S}_{ij}^{u*(o)} + \hat{S}_{ij}^{u*(c)} + \bar{S}_{ij}^{u*} \quad (32)$$

The components $\underline{S}^{u*(o)}$, $\underline{S}^{u*(c)}$, $\hat{S}^{u*(o)}$, $\hat{S}^{u*(c)}$ and \bar{S}_{ij}^{u*} for any given modification of the current stress $\underline{\sigma}$, can be estimated from Equations (17), (19), (25), (27) and (29). Obviously, they differ from the appropriate counterparts in Equation (31).

In general, the number of mesocracks

$$N_m = N_m^{(o)} + N_m^{(c)} = \text{const.} \quad (33)$$

and the number of existing kinks

$$N_k = 2(\hat{N}_m^{(o)} + \hat{N}_m^{(c)}) = \text{const.} \quad (34)$$

although, in particular cases of the current state $\underline{\sigma}$, small changes are possible. Assumptions (33) and (34) are valid particularly for the state preceding the final failure where the so-called saturation state of mesocracks is reached [12].

The constitutive equations for unloading are similar to Equation (7) and the values of recoverable strains are equal:

$$\underline{\epsilon}^r = \underline{S}^u(\underline{\sigma}, \underline{\omega}) \cdot \underline{\sigma} \quad (35)$$

5. PHENOMENOLOGICAL DESCRIPTION OF THE DAMAGE STATE IN THE MATERIAL

Usually, micromechanically based material models evaluate the state of damage by introduction parameters that are connected with a density of straight slits and their dimensions (e.g., Reference [30]). There are good measures for early stages of the material deformation, where no crack deflection occurs.

As was noted above (Sections 3 and 4), in the case of multi-axial stress $\underline{\sigma}$, the state of solid fissuration is more complicated. Therefore, it seems reasonable to introduce another measure of internal degradation, describing all effects appearing within the unit cell subjected to the loading process.

The easiest method proposed for uniaxial tension [31] is damage characteriza-

tion just by unloading modulus E^* :

$$\omega = 1 - \frac{E^*}{E^0} \quad (36)$$

where E^0 is the initial Young's modulus. As was pointed out in Reference [2], the advantage of such a representation results from the fact that it "can be measured in a very simple and unambiguous manner".

A simple generalization of the concept in Equation (36) was proposed in Reference [12] for the description of the uniaxial compression process of semi-brittle ceramics and the two-dimensional damage state. According to the "hypothesis of stress equivalence," one can postulate the following damage definition:

$$\omega_i = \frac{\Delta \epsilon_i^r}{\epsilon_i^r}, \quad i = 1, 2, 6 \quad (37)$$

where ϵ_i^r is the total strain recoverable during unloading, and $\Delta \epsilon_i^r$ is its part associated with crack existence. With definitions (32) and (35), $\Delta \epsilon_i^r$ can be calculated as:

$$\Delta \underline{\epsilon}^r = (\underline{S}^u - \underline{S}^0) \cdot \underline{\sigma} \quad (38)$$

and then Equation (37) takes the final form:

$$\omega_i = \frac{(S_{ij}^u - S_{ij}^0)\sigma_j}{S_{ij}^u \sigma_j}, \quad i = 1, 2, 6 \quad (39)$$

It is worth pointing out that definition (37) allows a deep physical interpretation of all components of the tensor $\underline{\omega}$ —not only ω_1 and ω_2 , but also ω_6 . It shows that "damage" contains numerous complicated mechanisms, as described in Sections 3 and 4.

6. CONCLUDING REMARKS

This paper discusses the construction of constitutive equations for the quasi-static deformation process of semi-brittle materials from the onset to the state preceding final failure. The most important mechanisms influencing the overall compliance tensor were specified. Many effects, such as crack interaction and bridging phenomenon by coarse grains, were not taken into account; they have greater significance on the material behaviour at the final failure and post-critical stages [20].

The simple connection between mesomechanical and phenomenological modelling of damage is possible. The generalization of the damage measurement idea by unloading compliance allows one to follow the whole non-linear unloading process, specifying all mechanisms contained in it [22].

ACKNOWLEDGEMENTS

The author gratefully acknowledges the financial support rendered by the research grant from the German Research Society's (DFG), project No. 218/1-2 on dynamic testing of high strength ceramics. Thanks also to Prof. Jerzy Najar for fruitful discussion.

APPENDIX A

The state of strain associated with the opened, straight crack (of length $2c$) existence considered in the local coordinate system (Figure 1) can be described:

$$f_d^{(o)} \epsilon'_{ij} = \frac{1}{2A} \int_{-c}^c \{n'_i [u'_j] + n'_j [u'_i]\} dx'_i \quad (A1)$$

where n'_i are the components of the unit vector, which is normal to the crack surface, u'_i are the components of the crack displacement vector, and $f_d^{(o)}$ is the opened crack area density. In our case, $n'_1 = 0, n'_2 = 1$ and

$$u'_1 = 4\sqrt{c^2 - x_1'^2} (\sigma'_6/E_0), \quad u'_2 = 4\sqrt{c^2 - x_1'^2} (\sigma'_2/E_0) \quad (A2)$$

Taking the above into account, Equation (A1) gives only one component:

$$f_d^{(o)} \begin{pmatrix} \epsilon'_1 \\ \epsilon'_2 \\ \epsilon'_6 \end{pmatrix} = \frac{2\pi c^2}{AE_0} \begin{pmatrix} 0 \\ \sigma'_2 \\ \sigma'_6 \end{pmatrix} \quad (A3)$$

Rewriting Equation (A3) in terms of the global coordinate system and using a simple orthogonal transformation [1,7,12],

$$[g] = \begin{bmatrix} \cos^2 \phi & \sin^2 \phi & \sin 2\phi \\ \sin^2 \phi & \cos^2 \phi & -\sin 2\phi \\ \frac{1}{2} \sin 2\phi & \frac{1}{2} \sin 2\phi & \cos 2\phi \end{bmatrix} \quad (A4)$$

we gain the influence of one slit on the overall material response:

$$f_d^{(o)} \begin{pmatrix} \epsilon_1 \\ \epsilon_2 \\ \epsilon_6 \end{pmatrix} = \frac{2\pi c^2}{AE_0} \begin{pmatrix} M_{11}^{(o)} & M_{12}^{(o)} & M_{16}^{(o)} \\ M_{21}^{(o)} & M_{22}^{(o)} & M_{26}^{(o)} \\ M_{61}^{(o)} & M_{62}^{(o)} & M_{66}^{(o)} \end{pmatrix} \begin{pmatrix} \sigma_1 \\ \sigma_2 \\ 0 \end{pmatrix} \quad (\text{A5})$$

where matrix $M_{ij}^{(o)}$ can be expressed

$$\{M_{ij}^{(o)}\} = \begin{pmatrix} \sin^2 \phi (2 - 3 \cos^2 \phi) & 3 \sin^2 \phi \cos^2 \phi & 0 \\ \cos^2 \phi (1 - \cos^2 \phi) & \cos^2 \phi (1 + \cos^2 \phi) & 0 \\ -\frac{1}{2} \sin 2\phi (1 + 2 \sin^2 \phi) & -\frac{1}{2} \sin 2\phi (1 + 2 \cos^2 \phi) & 0 \end{pmatrix} \quad (\text{A6})$$

In the case when grains (of diameter D) are not equal and $N_m^{(o)}$ mesocracks occupy straight segments of crystals ($c = D/4$) in the unit cell, the overall compliance can be finally estimated by an averaging procedure

$$S_{ij}^{*(o)} = \frac{2\pi}{AE_0} N_m^{(o)} \int_{\phi_{c1}^{(o)}}^{\phi_{c2}^{(o)}} \int_{D_m}^{D_M} M_{ij}^{(o)} \left(\frac{D}{4}\right)^2 p_1(\phi) p_2(D) dD d\phi \quad (\text{A7})$$

where $p_1(\phi)$ and $p_2(D)$ are the inclination of the mesocrack and the grain size distribution functions, respectively. For homogeneous distributions, p_1 and p_2 are equal:

$$p_1(\phi) = \frac{1}{\phi_{c2}^{(o)} - \phi_{c1}^{(o)}}; \quad p_2(D) = \frac{1}{D_M - D_m} \quad (\text{A8})$$

$\phi_{c1}^{(o)} < \sigma^{(o)} < \phi_{c2}^{(o)}$ denotes the fan of $N_m^{(o)}$ cracks.

APPENDIX B

The strains created by the closed, straight slit will be calculated according to Equation (A1). Case (A2) takes the form:

$$u_1' = 4\sqrt{c^2 - x_1'^2} (\tau_s/E_0), \quad u_2' = 0 \quad (\text{B1})$$

and Equation (A3), appropriately (see Reference [12]):

$$f_d^{(c)} \begin{pmatrix} \epsilon'_1 \\ \epsilon'_2 \\ \epsilon'_6 \end{pmatrix} = \frac{2\pi c^2}{AE_0} \begin{pmatrix} 0 \\ 0 \\ \tau_s \end{pmatrix} \quad (\text{B2})$$

where $f_d^{(c)}$ is the closed crack area density.

Performing a similar procedure to that in Appendix A, one can obtain

$$f_d^{(c)} \begin{pmatrix} \epsilon_1 \\ \epsilon_2 \\ \epsilon_6 \end{pmatrix} = \frac{2\pi c^2}{AE_0} \begin{pmatrix} M_{11}^{(c)} & M_{12}^{(c)} & M_{16}^{(c)} \\ M_{21}^{(c)} & M_{22}^{(c)} & M_{26}^{(c)} \\ M_{61}^{(c)} & M_{62}^{(c)} & M_{66}^{(c)} \end{pmatrix} \begin{pmatrix} \sigma_1 \\ \sigma_2 \\ 0 \end{pmatrix} \quad (\text{B3})$$

where matrix $M_{ij}^{(c)}$ can be expressed

$$\{M_{ij}^{(c)}\} = \begin{pmatrix} -\frac{1}{4} \sin^2 2\phi + \mu \sin^3 \phi \cos \phi & \frac{1}{4} \sin^2 2\phi - \mu \sin \phi \cos^3 \phi & 0 \\ \frac{1}{4} \sin^2 2\phi + \mu \sin^3 \phi \cos \phi & -\frac{1}{4} \sin^2 2\phi + \mu \sin \phi \cos^3 \phi & 0 \\ \frac{1}{4} \sin 4\phi + \mu \sin^2 \phi \cos 2\phi & -\frac{1}{4} \sin 4\phi + \mu \cos^2 \phi \cos 2\phi & 0 \end{pmatrix} \quad (\text{B4})$$

In the case where grains (of diameter D) are not equal and $N_m^{(c)}$ mesocracks occupy straight segments of crystals ($c = D/4$) in the unit cell, the overall compliance can be finally estimated by an averaging procedure

$$S_{ij}^{*(c)} = \frac{2\pi}{AE_0} N_m^{(c)} \int_{\phi_{c1}^{(c)}}^{\phi_{c2}^{(c)}} \int_{D_m}^{D_M} M_{ij}^{(c)} \left(\frac{D}{4}\right)^2 p_1(\phi) p_2(D) dD d\phi \quad (\text{B5})$$

where the function $p_1(\phi)$ is equal

$$p_1(\phi) = \frac{1}{\phi_{c2}^{(c)} - \phi_{c1}^{(c)}} \quad (\text{B6})$$

and $p_2(D)$ is defined by Equation (A8). $\phi_{c1}^{(c)} < \phi^{(c)} < \phi_{c2}^{(c)}$ denotes the fan of $N_m^{(c)}$ cracks.

APPENDIX C

A particular discussion of the strain state associated with the kink development was presented in Reference [7]. For our purposes, let us consider the straight crack PQ shown in Figure 3. In the local coordinate system x'_1, x'_2 , we have the following strain components:

$$\{\epsilon'_i\} = \begin{Bmatrix} \epsilon'_1 \\ \epsilon'_2 \\ \epsilon'_6 \end{Bmatrix} = \begin{Bmatrix} 0 \\ \frac{1}{2}\bar{l}(\bar{b} \sin \theta + \bar{d} \cos \theta) \\ \frac{1}{2}\bar{l}(\bar{b} \cos \theta - \bar{d} \sin \theta) \end{Bmatrix} \quad (C1)$$

where $\bar{l} = l/c$ is the dimensionless length of the crack, whereas \bar{b} is the mesocrack PP' dimensionless slip

$$\bar{b} = \frac{1}{2c} \int_{-c}^c u'_1 dx'_1 = \frac{\pi}{E_0} \sigma'_6 \quad (C2)$$

\bar{d} is the dimensionless averaged opening of the mesocrack PP'

$$\bar{d} = \frac{1}{2c} \int_{-c}^c u'_2 dx'_1 = \frac{\pi}{E_0} \sigma'_2 \quad (C3)$$

Introducing Equations (C2) and (C3) to (C1) and using (A1), we gain

$$\hat{f}_d^{(o)} \epsilon'_i = \frac{\pi \bar{l}}{2E_0} (\delta_{2i} (\delta_{6j} \sin \theta + \delta_{2j} \cos \theta) + \delta_{6i} (\delta_{6j} \cos \theta - \delta_{2j} \sin \theta)) \sigma'_j \quad (C4)$$

where $\hat{f}_d^{(o)}$ is the surface area density of the opened mesocracks. Using the transformation rules:

$$\epsilon_i = \epsilon'_i \bar{g}_{ii} \quad (C5a)$$

$$\sigma'_i = \sigma_k g_{ik} \quad (C5b)$$

where \bar{g}_{ii} is the matrix similar to Equation (A4):

$$[\bar{g}] = \begin{bmatrix} \cos^2(\theta + \phi) & \sin^2(\theta + \phi) & \sin 2(\theta + \phi) \\ \sin^2(\theta + \phi) & \cos^2(\theta + \phi) & -\sin 2(\theta + \phi) \\ -\frac{1}{2} \sin 2(\theta + \phi) & \frac{1}{2} \sin(\theta + \phi) & \cos 2(\theta + \phi) \end{bmatrix} \quad (C6)$$

Equation (C4) takes the following form for one slit in the global coordinate system:

$$\hat{f}_d^{(\circ)} \begin{pmatrix} \epsilon_1 \\ \epsilon_2 \\ \epsilon_6 \end{pmatrix} = \frac{\pi \bar{l}}{2E_0} \begin{pmatrix} \hat{M}_{11}^{(\circ)} & \hat{M}_{12}^{(\circ)} & \hat{M}_{16}^{(\circ)} \\ \hat{M}_{21}^{(\circ)} & \hat{M}_{22}^{(\circ)} & \hat{M}_{26}^{(\circ)} \\ \hat{M}_{61}^{(\circ)} & \hat{M}_{62}^{(\circ)} & \hat{M}_{66}^{(\circ)} \end{pmatrix} \begin{pmatrix} \sigma_1 \\ \sigma_2 \\ 0 \end{pmatrix} \quad (C7)$$

$$\{\hat{M}_{ij}^{(\circ)}\} = \begin{pmatrix} \sin \phi \cos(2\theta) \sin(\theta + \phi) & \cos \phi \sin(2\theta) \sin(\theta + \phi) & 0 \\ -\sin \phi \sin(2\theta) \cos(\theta + \phi) & \cos \phi \cos(2\theta) \cos(\theta + \phi) & 0 \\ -\sin \phi \cos(3\theta + \phi) & -\cos \phi \sin(3\theta + \phi) & 0 \end{pmatrix} \quad (C8)$$

In the case where grains (of diameter D) are not equal and $\hat{N}_m^{(\circ)}$ mesocracks occupy straight segments of crystals ($c = D/4$) in the unit cell, the overall compliance can be finally estimated by an averaging procedure

$$\hat{S}_{ij}^{*(\circ)} = \frac{\pi}{E_0} \hat{N}_m^{(\circ)} \int_{\bar{l}_{k_1}^{(\circ)}}^{\bar{l}_{k_2}^{(\circ)}} p_{k_1}(\bar{l}) \int_{\theta_{k_1}^{(\circ)} + \phi_{k_1}^{(\circ)}}^{\theta_{k_2}^{(\circ)} + \phi_{k_2}^{(\circ)}} \hat{M}_{ij}^{(\circ)} p_{k_2}(\theta + \phi) \bar{l} d\bar{l} d(\theta + \phi) \quad (C9)$$

In Equation (C9), p_{k_1} and p_{k_2} are the tension crack length and their inclination angle distribution functions, respectively

$$p_{k_1}(\bar{l}) = \frac{1}{\bar{l}_{k_2}^{(\circ)} - \bar{l}_{k_1}^{(\circ)}} \quad (C10)$$

$$p_{k_2}(\theta + \phi) = \frac{1}{(\theta_{k_2}^{(\circ)} + \phi_{k_2}^{(\circ)}) - (\theta_{k_1}^{(\circ)} + \phi_{k_1}^{(\circ)})} \quad (C11)$$

$\bar{l}_{k_1}^{(\circ)} \leq \bar{l} \leq \bar{l}_{k_2}^{(\circ)}$ characterizes the fan of the length, whereas $\theta_{k_1}^{(\circ)} + \phi_{k_1}^{(\circ)} \leq \theta + \phi \leq \theta_{k_2}^{(\circ)} + \phi_{k_2}^{(\circ)}$ characterizes the fan of kinked crack inclination.

APPENDIX D

In the case of closed mesocracks, Equation (C2) becomes (see Reference [12])

$$\bar{b} = \frac{1}{2c} \int_{-c}^c u'_i dx'_i = \frac{\pi}{E_0} \tau_s \tag{D2}$$

whereas

$$\bar{d} = 0 \tag{D3}$$

Introducing Equations (D2) and (D3) to (C1) and using (A), we gain

$$\hat{f}_d^{(c)} \epsilon'_i = \frac{\pi \bar{l}}{2E_0} (\delta_{2i} \sin \theta + \delta_{6i} \cos \theta) \tau_s \tag{D4}$$

where $\hat{f}_d^{(c)}$ is the surface area density of the closed mesocracks. Performing the same transformation as in Appendix C, the state of strain in the global coordinate system is

$$\hat{f}_d^{(c)} \begin{pmatrix} \epsilon_1 \\ \epsilon_2 \\ \epsilon_6 \end{pmatrix} = \frac{\pi \bar{l}}{2E_0} \begin{pmatrix} \hat{M}_{11}^{(c)} & \hat{M}_{12}^{(c)} & \hat{M}_{16}^{(c)} \\ \hat{M}_{21}^{(c)} & \hat{M}_{22}^{(c)} & \hat{M}_{26}^{(c)} \\ \hat{M}_{61}^{(c)} & \hat{M}_{62}^{(c)} & \hat{M}_{66}^{(c)} \end{pmatrix} \begin{pmatrix} \sigma_1 \\ \sigma_2 \\ 0 \end{pmatrix} \tag{D5}$$

and the matrix $\hat{M}_{ij}^{(c)}$, appropriately

$$\begin{aligned} & \{\hat{M}_{ij}^{(c)}\} \\ & = \begin{pmatrix} \sin^2 \phi \cos \phi \sin (\theta + \phi) [\text{ctg } \phi - \mu] & \cos^3 \phi \sin (\theta + \phi) [\text{tg } \phi - \mu] & 0 \\ -\sin^3 \phi \cos (\theta + \phi) [\text{ctg } \phi - \mu] & \sin \phi \cos^2 \phi \cos (\theta + \phi) [\text{tg } \phi - \mu] & 0 \\ -\sin^2 \phi \cos (\theta + 2\phi) [\text{ctg } \phi - \mu] & \cos^2 \phi \cos (\theta + 2\phi) [\text{tg } \phi - \mu] & 0 \end{pmatrix} \end{aligned} \tag{D6}$$

Finally, the compliance tensor has the following form when grains (of diameter D) in the unit cell are not equal and $\hat{N}_m^{(c)}$ closed mesocracks occupy straight segments of crystals ($c = D/4$)

$$\hat{S}_{ij}^{*(c)} = \frac{\pi}{E_0} \hat{N}_m^{(c)} \int_{\theta_{k_1}^{(c)}}^{\theta_{k_2}^{(c)}} p_{k_1}(\bar{l}) \int_{\theta_{k_1}^{(c)} + \phi_{k_1}^{(c)}}^{\theta_{k_2}^{(c)} + \phi_{k_2}^{(c)}} \hat{M}_{ij}^{(c)} p_{k_2}(\theta + \phi) \bar{l} d\bar{l} d(\theta + \phi) \tag{D7}$$

$\bar{l}_{k_1}^{(c)} \leq \bar{l} \leq \bar{l}_{k_2}^{(c)}$ characterizes the fan of the length, whereas $\theta_{k_1}^{(c)} + \phi_{k_1}^{(c)} \leq \theta + \phi \leq \theta_{k_2}^{(c)} + \phi_{k_2}^{(c)}$ characterizes the fan of kinked crack inclination.

$$p_{k_1}(\bar{l}) = \frac{1}{\bar{l}_{k_2}^{(c)} - \bar{l}_{k_1}^{(c)}} \tag{D8}$$

$$p_{k_2}(\theta + \phi) = \frac{1}{(\theta_{k_2}^{(c)} + \phi_{k_2}^{(c)}) - (\theta_{k_1}^{(c)} + \phi_{k_1}^{(c)})} \tag{D9}$$

with the assumption of homogeneous distribution of defects.

APPENDIX E

The closing or opening process of the tension crack PQ depends on the actual state of the external stress. According to Equations (C5b), (A2) and (A1), the strain can be calculated:

$$f_d^{(k)} \begin{pmatrix} \epsilon'_1 \\ \epsilon'_2 \\ \epsilon'_6 \end{pmatrix} = \frac{\pi \bar{l}^2 c^2}{2AE_0} \begin{pmatrix} 0 \\ \sigma'_2 \\ \sigma'_6 \end{pmatrix} \tag{E1}$$

where $f_d^{(k)}$ is the kink density in the unit cell. After transformation Equation (E1) to the global coordinate system:

$$f_d^{(k)} \begin{pmatrix} \epsilon_1 \\ \epsilon_2 \\ \epsilon_6 \end{pmatrix} = \frac{\pi \bar{l}^2 c^2}{2AE_0} \begin{pmatrix} \bar{M}_{11} & \bar{M}_{12} & \bar{M}_{16} \\ \bar{M}_{21} & \bar{M}_{22} & \bar{M}_{26} \\ \bar{M}_{61} & \bar{M}_{62} & \bar{M}_{66} \end{pmatrix} \begin{pmatrix} 0 \\ \sigma'_2 \\ \sigma'_6 \end{pmatrix} \tag{E2}$$

and

$$\{\bar{M}_{ij}\} = \begin{pmatrix} \sin^2(\theta + \phi) & 0 & 0 \\ 0 & \cos^2(\theta + \phi) & 0 \\ -\frac{1}{2} \sin 2(\theta + \phi) & -\frac{1}{2} \sin 2(\theta + \phi) & 0 \end{pmatrix} \tag{E3}$$

Then the total compliance for opened and closed mesocracks will be estimated as a sum of:

$$\bar{S}_{ij}^* = \frac{\pi D^2}{16AE_0} \left[\hat{N}_m^{(c)} \int_{\bar{l}_{k_1}^{(c)}}^{\bar{l}_{k_2}^{(c)}} p_{k_1}(\bar{l}) \int_{\theta_{k_1}^{(c)} + \phi_{k_1}^{(c)}}^{\theta_{k_2}^{(c)} + \phi_{k_2}^{(c)}} \bar{M}_{ij} p_{k_2}(\theta + \phi) \bar{l}^2 d\bar{l} d(\theta + \phi) \right]$$

$$+ \hat{N}_m^{(c)} \int_{\gamma_{k_1}^{(c)}}^{\gamma_{k_2}^{(c)}} p_{k_1}(\bar{l}) \int_{\theta_{k_1}^{(c)} + \phi_{k_1}^{(c)}}^{\theta_{k_2}^{(c)} + \phi_{k_2}^{(c)}} \bar{M}_{ij} p_{k_2}(\theta + \phi) \bar{l}^2 d\bar{l} d(\theta + \phi) \Big] \quad (E4)$$

The distribution functions p_{k_1} and p_{k_2} are similar to Equations (C10), (C11) and (D8), (D9).

REFERENCES

1. Horii, H. and S. Nemat-Nasser. 1983. "Overall Moduli of Solids with Microcracks: Load Induced Anisotropy," *J. Mech. Phys. Solids*, 31:155-171.
2. Krajcinovic, D. and D. Sumarac. 1989. "A Mesomechanical Model for Brittle Deformation Process," *J. Appl. Mech.*, 56:51-56.
3. Krajcinovic, D. 1989. "Damage Mechanics," *Mech. Mater.*, 8:117-197.
4. Lemaitre, J. and J. L. Chaboche. 1985. *Mechanique des Materiaux Solides*. Paris: Dunod.
5. Chow, C. L. and T. J. Lu. 1989. "On Evolution Laws of Anisotropic Damage," *Eng. Fract. Mech.*, 34:679-701.
6. Lu, T. J. and C. L. Chow. 1990. "On Constitutive Equations of Inelastic Solids with Anisotropic Damage," *Theor. Appl. Fract. Mech.*, 14:187-218.
7. Nemat-Nasser, S. and M. Obata. 1988. "A Microcrack Model of Dilatancy in Brittle Materials," *J. Appl. Mech.*, 55:24-35.
8. Najjar, J. 1987. "Continuous Damage of Brittle Solids," in *Continuum Damage Mechanics. Theory and Applications*, D. Krajcinovic and J. Lemaitre, eds., Wien: Springer, pp. 233-294.
9. Sadowski, T. 1991. "Deformation Damage Theory of Materials and Its Application to the Analysis of the Deformation Process of Square Plates," *Arch. Appl. Mech.*, 61:449-461.
10. Stoimirovic, A., D. Krajcinovic and T. Sadowski. 1987. "Constitutive Model for Polycrystalline MgO Ceramics," in *Constitutive Modelling for Nontraditional Materials*, V. Stokes and D. Krajcinovic, eds., ASME Publ., AMD-Vol. 85, pp. 175-184.
11. Krajcinovic, D. and A. Stoimirovic. 1990. "Deformation Process in Semibrittle Polycrystalline Ceramics," *Int. J. Fracture*, 42:73-86.
12. Sadowski, T. 1994. "Modelling of Semi-Brittle MgO Ceramic Behaviour under Compression State," to appear in *Mech. Mater.*
13. Mura, T. 1982. *Micromechanics of Defects in Solids*. The Hague, Netherlands, Boston: Martinus Nijhoff.
14. Kunin, I. 1983. *Elastic Media with Microstructure II, Three-Dimensional Models*. Berlin: Springer-Verlag.
15. Kreher, W. and W. Pompe. 1989. *Internal Stress in Heterogeneous Solids*. Berlin: Akademie Verlag.
16. Davidge, W. 1979. *Mechanical Behaviour of Ceramics*. Cambridge, U.K.: Cambridge University Press.
17. Stokes, R. J. 1972. "Microscopic Aspects of Fracture in Ceramics," in *Fracture, Vol. VII*, H. Liebovitz, ed., New York: Academic Press, pp. 157-241.
18. Papadopoulos, G. A., V. N. Kytopoulos and T. Sadowski. 1994. "Experimental Study of Fracture Process in MgO Polycrystalline Ceramics," report, *The Fourth International Symposium on Brittle Matrix Composites*, Warsaw, September 1994 (in print).
19. Litewka, A. 1985. "Effective Material Constants for Orthotropically Damaged Elastic Solids," *Arch. Mech.*, 37:631-642.
20. Sadowski, T. 1994. "General Formulation of the Constitutive Relations for Semi-Brittle Materials" (in preparation).

21. Krajcinovic, D., D. Sumarac and K. Mallick. 1992. "Elastic Parameters of Brittle, Elastic Solids Containing Slits—Critical State," *Int. J. Dam. Mech.*, 1:386–403.
22. Sadowski, T. 1994. "Mechanical Response of Semi-Brittle Ceramics Subjected to Tension-Compression State. Part II: Description of Deformation Process," *Int. J. Dam. Mech.* (in print).
23. Krell, A. and P. Blank. 1992. "Inherent Reinforcement of Ceramic Microstructures by Grain Boundary Engineering," *J. Europ. Ceram. Soc.*, 9:309–322.
24. Horii, H. and S. Nemat-Nasser. 1986. "Brittle Failure in Compression: Splitting, Faulting and Brittle-Ductile Transition," *Phil. Trans. R. Soc. Lond. A*, 319:337–374.
25. Evans, A. G. 1990. "Perspective on the Development of High-Toughness Ceramics," *J. Am. Ceram. Soc.*, 73:187–206.
26. Ortiz, M. 1988. "Microcrack Coalescence and Microscopic Crack Growth Initiation in Brittle Solids," *Int. J. Solids Struct.*, 24:231–250.
27. Kachanov, M., E. Montagut and J. Laures. 1990. "Mechanics of Crack-Microcrack Interaction," *Mech. Mat.*, 10:59–71.
28. Chow, C. L. and T. J. Lu. 1991. "A Continuum Damage Mechanics Approach to Crack Tip Shielding in Brittle Solids," *Int. J. Fract.*, 50:79–114.
29. Sadowski, T. 1984. "Continuous Damage of Elastic-Brittle and Elastic-Plastic Materials in Uniaxial State of Stress," *Eng. Trans.*, 32:499–521.
30. Budiansky, B. and R. O'Connell. 1976. "Elastic Moduli of a Cracked Solid," *Int. J. Solids Struct.*, 13:81–97.
31. Lemaitre, J. and J. L. Chaboche. 1978. "Aspect Phenomenologique de la Rupture par Endommagement," *J. Mec. Appl.*, 2:317–365.